Study of $X(5568)$ in a unitary coupled-channel approximation of $B\bar{K}$ and $B_s\pi$

Bao-Xi Sun(孙宝玺)[1,2;1)] Fang-Yong Dong(董方勇)[1] Jing-Long Pang(庞景龙)[2]

[1] College of Applied Sciences, Beijing University of Technology, Beijing 100124, China
[2] Department of Physics, Peking University, Beijing 100871, China

Abstract: The potential of the B meson and the pseudoscalar meson is constructed up to the next-to-leading order Lagrangian, and then the $B\bar{K}$ and $B_s\pi$ interaction is studied in the unitary coupled-channel approximation. A resonant state with a mass about 5568 MeV and $J^P=0^+$ is generated dynamically, which can be associated with the $X(5568)$ state announced by the D0 Collaboration recently. The mass and the decay width of this resonant state depend on the regularization scale in the dimensional regularization scheme, or the maximum momentum in the momentum cutoff regularization scheme. The scattering amplitude of the vector B meson and the pseudoscalar meson is calculated, and an axial-vector state with a mass near 5620 MeV and $J^P=1^+$ is produced. Their partners in the charm sector are also discussed.

Keywords: chiral Lagrangian, meson-meson interactions, exotic mesons

PACS: 12.39.Fe, 13.75.Lb, 14.40.Rt **DOI:** 10.1088/1674-1137/41/7/074104

1 Introduction

The D0 Collaboration recently announced the discovery of a new state, $X(5568)$, as a narrow peak in the $B_s^0\pi^\pm$ invariant mass distribution with significance of 5.1σ, based on 10.4 fb^{-1} of $p\bar{p}$ collisions at $\sqrt{s}=1.96$ TeV [1]. The $X(5568)$ has a mass of $M=5567.8\pm2.9^{+0.9}_{-1.9}$ MeV and a decay width of $\Gamma=21.9\pm6.4^{+5.0}_{-2.5}$ MeV. This discovery implies that $X(5568)$ might be composed of two quarks and two antiquarks, of four different flavors, b, s, u, and d, and thus it might be a candidate for an exotic tetraquark state. Along with this clue, many theorists try to explain its properties at the quark level, or treat it as a molecule state of a B meson and a pseudoscalar meson [2–22]. However, some theoretical works do not support the existence of the $X(5568)$ state [23–30]. Recently, a negative result has been reported by the LHCb Collaboration [31]. They claim that no significant excess has been found, based on the data sample recorded with the LHCb detector corresponding to 3 fb^{-1} of pp collision data at $\sqrt{s}=7\sim8$ TeV. In addition, the CMS Collaboration have searched for resonance-like structures in the $B_s^0\pi^\pm$ invariant mass spectrum using an integrated luminosity of 19.7 fb^{-1} of proton-proton collisions at $\sqrt{s}=8$ TeV, and they report that no hint of the $X(5568)$ particle is shown [32].

In the present work, the interaction of the B meson and the pseudoscalar meson is studied in chiral perturbation theory. We calculate the interaction potentials up to next-to-leading order correction, and then solve the Bethe-Salpeter equation in the unitary coupled-channel approximation. A resonant state with a mass of about 5568 MeV is generated dynamically in the $B\bar{K}$ and $B_s\pi$ channels, and is assumed to be associated with the $X(5568)$ particle. Thus, we think that the $X(5568)$ state has a quantum number $J^P=0^+$.

This article is organized as follows. In Section 2, the effective chiral Lagrangian is given. In Section 3, the potential of the B meson and the pseudoscalar meson up to the next-to-leading order correction is constructed according to the Lagrangian in Section 2. In Section 4, the Bethe-Salpeter equation is discussed in the unitary coupled-channel approximation. The calculation results for the $B_s\pi$ and $B\bar{K}$ channels are summarized in Section 5. In Section 6, the coupled channels $B_s^*\pi$ and $B^*\bar{K}$ are studied in the unitary coupled-channel approximation, and a resonant state with a mass near 5620 MeV and $J^P=1^+$ is generated dynamically. In Section 7, the corresponding charm sectors are analyzed in the unitary coupled-channel approximation. Finally, a summary is given in Section 8.

2 Chiral Lagrangian up to next-to-leading order

For the B meson, the triplets take the forms of $P=(B^-,\bar{B}^0,\bar{B}_s^0)$ and $P^\dagger=(B^+,B^0,B_s^0)$, and for the

Received 04 January 2017, Revised 05 March 2017

1) E-mail: sunbx@bjut.edu.cn

vector B* meson, we have $P^*_\mu=(\mathrm{B}^{*-},\bar{\mathrm{B}}^{*0},\bar{\mathrm{B}}^{*0}_{\mathrm{s}})_\mu$ and $P^{*\dagger}_\mu=(\mathrm{B}^{*+},\mathrm{B}^{*0},\mathrm{B}^{*0}_{\mathrm{s}})_\mu$. The leading order chiral Lagrangian describing the interactions of the B meson with the pseudoscalar meson can be written as:

$$\begin{aligned}\mathcal{L}^{(1)} =& \langle\mathcal{D}_\mu P\mathcal{D}^\mu P^\dagger\rangle - m_P^2\langle PP^\dagger\rangle\\ &-\langle\mathcal{D}_\mu P^{*\nu}\mathcal{D}^\mu P^{*\dagger}_\nu\rangle+m^2_{P^*}\langle P^{*\nu}P^{*\dagger}_\nu\rangle,\end{aligned}\qquad(1)$$

where m_P and m_{P^*} are the masses of the B and vector B* meson, respectively, and $\langle...\rangle$ denotes the trace in $SU(3)$ flavor space. The chiral covariant derivative is defined as

$$\mathcal{D}_\mu P_a=\partial_\mu P_a-\Gamma^{ba}_\mu P_b,\quad \mathcal{D}^\mu P^\dagger_a=\partial^\mu P^\dagger_a-\Gamma^\mu_{ab}P^\dagger_b,\qquad(2)$$

where the vector current $\Gamma_\mu=\frac{1}{2}(\xi^\dagger\partial_\mu\xi+\xi\partial_\mu\xi^\dagger)$ and $\xi^2=\exp(\mathrm{i}\Phi/f_0)$, with f_0 being the decay constant of the pseudoscalar meson and Φ the octet of pseudoscalar mesons:

$$\Phi=\sqrt{2}\begin{pmatrix}\frac{\pi^0}{\sqrt{2}}+\frac{\eta}{\sqrt{6}} & \pi^+ & K^+\\ \pi^- & -\frac{\pi^0}{\sqrt{2}}+\frac{\eta}{\sqrt{6}} & K^0\\ K^- & \bar{K}^0 & -\frac{2}{\sqrt{6}}\eta\end{pmatrix}.\qquad(3)$$

Similarly, the covariant next-to-leading order (NLO) terms of the effective Lagrangian are constructed:

$$\begin{aligned}\mathcal{L}^{(2)} =& -2[c_0\langle PP^\dagger\rangle\langle\chi_+\rangle-c_1\langle P\chi_+P^\dagger\rangle-c_2\langle PP^\dagger\rangle\langle u^\mu u_\mu\rangle\\ &-c_3\langle Pu^\mu u_\mu P^\dagger\rangle+\frac{c_4}{m_P^2}\langle\mathcal{D}_\mu P\mathcal{D}_\nu P^\dagger\rangle\langle\{u^\mu,u^\nu\}\rangle\\ &+\frac{c_5}{m_P^2}\langle\mathcal{D}_\mu P\{u^\mu,u^\nu\}\mathcal{D}_\nu P^\dagger\rangle\\ &+\frac{c_6}{m_P^2}\langle\mathcal{D}_\mu P[u^\mu,u^\nu]\mathcal{D}_\nu P^\dagger\rangle]\\ &+2[\tilde{c}_0\langle P^*_\mu P^{*\mu\dagger}\rangle\langle\chi_+\rangle-\tilde{c}_1\langle P^*_\mu\chi_+P^{*\mu\dagger}\rangle\\ &-\tilde{c}_2\langle P^*_\nu P^{*\nu\dagger}\rangle\langle u^\mu u_\mu\rangle-\tilde{c}_3\langle P^*_\nu u^\mu u_\mu P^{*\nu\dagger}\rangle\\ &+\frac{\tilde{c}_4}{m^2_{P^*}}\langle\mathcal{D}_\mu P^*_\alpha\mathcal{D}_\nu P^{*\alpha\dagger}\rangle\langle\{u^\mu,u^\nu\}\rangle\\ &+\frac{\tilde{c}_5}{m^2_{P^*}}\langle\mathcal{D}_\mu P^*_\alpha\{u^\mu,u^\nu\}\mathcal{D}_\nu P^{*\alpha\dagger}\rangle\\ &+\frac{\tilde{c}_6}{m^2_{P^*}}\langle\mathcal{D}_\mu P^*_\alpha[u^\mu,u^\nu]\mathcal{D}_\nu P^{*\alpha\dagger}\rangle],\end{aligned}\qquad(4)$$

where $u_\mu=i(\xi^\dagger\partial_\mu\xi-\xi\partial_\mu\xi^\dagger)$ is the axial current and $\chi_+=\xi^\dagger\mathcal{M}\xi^\dagger+\xi\mathcal{M}\xi$ with $\mathcal{M}=\mathrm{diag}(m^2_\pi,m^2_\pi,2m^2_K-m^2_\pi)$ [33, 34].

3 Potentials for B$\phi\to$Bϕ

For the process of $B_1(p_1)+\phi_1(k_1)\to B_2(p_2)+\phi_2(k_2)$, the leading order potential can be written as

$$V_{\mathrm{LO}}=\frac{1}{8f_0^2}C_{\mathrm{LO}}(s-u)\qquad(5)$$

with the Mandelstam variables $s=(k_1+p_1)^2=(k_2+p_2)^2$ and $u=(k_2-p_1)^2=(k_1-p_2)^2$. The coefficient C_{LO} for the different channels are listed in Table 1.

Table 1. Coefficients for the channels with $B=1$, $S=-1$ and $I=1$.

	C_{LO}	C_0	C_1	C_2	C_3	C_{41}	C_{42}	C_{51}	C_{52}
$\mathrm{B}\bar{\mathrm{K}}\to\mathrm{B}\bar{\mathrm{K}}$	0	$4m_K^2$	0	−2	0	−1	−1	0	0
$\mathrm{B}\bar{\mathrm{K}}\to\mathrm{B}^0_{\mathrm{s}}\pi^0$	−2	0	$4(m_K^2+m_\pi^2)$	0	2	0	0	0	2
$\mathrm{B}^0_{\mathrm{s}}\pi^0\to\mathrm{B}^0_{\mathrm{s}}\pi^0$	0	$4m_\pi^2$	0	−2	0	−1	−1	0	0

The next-to-leading order potential between the B meson and the pseudoscalar meson takes the following form:

$$\begin{aligned}V_{\mathrm{NLO}} =& \frac{1}{f_0^2}c_0C_0-\frac{1}{4f_0^2}c_1C_1\\ &+\frac{2}{f_0^2}c_2C_2k_1\cdot k_2+\frac{1}{f_0^2}c_3C_3k_1\cdot k_2\\ &-\frac{4}{m_P^2f_0^2}c_4*(C_{41}p_1\cdot k_1p_2\cdot k_2+C_{42}p_1\cdot k_2p_2\cdot k_1)\\ &-\frac{2}{m_P^2f_0^2}c_5*(C_{51}p_1\cdot k_1p_2\cdot k_2+C_{52}p_1\cdot k_2p_2\cdot k_1).\end{aligned}\qquad(6)$$

We shall discuss the amplitudes using the isospin formalism. The state with isospin $I=1$ can be written as

$$|B\bar{K},I=1\rangle=-\sqrt{\frac{1}{2}}B^+K^-+\sqrt{\frac{1}{2}}B^0\bar{K}^0,\qquad(7)$$

where the phase convention $|K^-\rangle=-\left|\frac{1}{2},-\frac{1}{2}\right\rangle$ for the isospin state has been used.

In the heavy-meson chiral perturbation theory, the leading order interaction between the B meson and the pseudoscalar meson can be written as

$$V_{\mathrm{LO}}=\frac{m_{\mathrm{B}}}{4f_0^2}C_{\mathrm{LO}}(E+E')\qquad(8)$$

with E and E' the energies of the initial and final pseudoscalar mesons, respectively.

The next-to-leading order interaction can be deduced from Eq. (6) in the heavy-meson approximation as

$$V_{\rm NLO}=-\frac{2}{f_0^2}c_0C_0+\frac{1}{2f_0^2}c_1C_1-\frac{4}{f_0^2}c_{24}C_2EE'-\frac{2}{f_0^2}c_{35}C_3EE', \tag{9}$$

where $c_{24}=c_2-2c_4$ and $c_{35}=c_3-2c_5$.

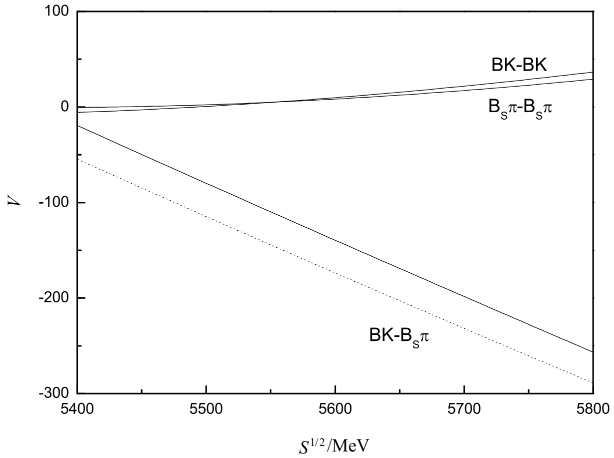

Fig. 1. The potential of the B meson and the pseudoscalar meson in the different channels. The solid lines denote the potentials in the leading order plus next-to-leading order approximation, and the dotted line stands for the leading order potential in the $B\bar{K}\rightarrow B_s\pi$ channel.

Up to the next-to-leading order Lagrangian, six low energy constants should be fixed. These low energy constants have been determined according to the lattice QCD data in Ref. [35], where the interaction between the pseudoscalar meson and the D meson is studied in a coupled-channel approximation of the chiral unitary theory, and the $D^*_{s0}(2317)$ is produced in the DK channel [34]. Their values are given in Table 2. Since the term multiplying c_6 is in fact of order $O(p^3)$, and it has a negligible effect on the dynamic generation of resonant states as long as c_6 is of a natural size, we set c_6 to be zero just as in Ref. [33, 34].

Table 2. Low energy constants for the pseudoscalar meson and D meson interaction.

	c_0	c_1	c_{24}	c_{35}
HQS UChPT	0.015	−0.214	−0.068	−0.011

The low energy constants c_0,...,c_6 in the interaction of the B meson and the pseudoscalar meson are related to those values in the case of the D meson and the pseudoscalar meson interaction. Up to corrections in $1/m_{\rm B}(m_{\rm D})$,

$$c_{i,B}/m_{\rm B}=c_{i,D}/m_{\rm D}, \tag{10}$$

where $m_{\rm B}$ =5331.9 MeV and $m_{\rm D}$ =1972.1 MeV are the average masses of the B and D mesons, respectively.

4 Unitary coupled-channel approximation of Bethe-Salpeter equation

The amplitude can be obtained by solving the Bethe-Salpeter equation in the S-wave approximation,

$$T(\sqrt{s})=[1-V_S(\sqrt{s})G(s)]^{-1}V_S(\sqrt{s}), \tag{11}$$

which is a function of the total energy $\sqrt{s}$ in the center-of-mass system. In Eq. (11), $G(s)$ is the propagator of a pseudoscalar meson and a B meson, and it can be calculated explicitly in a dimensional regularization scheme [36]:

$$\begin{aligned}G_l(s) &= {\rm i}\int\frac{{\rm d}^4q}{(2\pi)^4}\frac{1}{(P-q)^2-M_l^2+i\epsilon}\frac{1}{q^2-m_l^2+i\epsilon}\\ &= \frac{1}{16\pi^2}\Big\{a_l+\ln\frac{M_lm_l}{\mu^2}+\frac{m_l^2-M_l^2}{2s}\ln\frac{m_l^2}{M_l^2}\\ &\quad+\frac{\bar{q}_l}{\sqrt{s}}\left[\ln(s-(M_l^2-m_l^2)+2\bar{q}_l\sqrt{s})+\ln(s+(M_l^2-m_l^2)\right.\\ &\quad+2\bar{q}_l\sqrt{s})-\ln(-s+(M_l^2-m_l^2)+2\bar{q}_l\sqrt{s})\\ &\quad\left.-\ln(-s-(M_l^2-m_l^2)+2\bar{q}_l\sqrt{s})\right]\Big\},\end{aligned} \tag{12}$$

with μ the regularization scale, and a_l the subtraction constant.

In Eq. (12), $\bar{q}_l$ denotes the three-momentum of mesons in the center of mass system and is given by

$$\bar{q}_l=\frac{\sqrt{s-(M_l+m_l)^2}\sqrt{s-(M_l-m_l)^2}}{2\sqrt{s}}, \tag{13}$$

where M_l and m_l are the masses of the B meson and the pseudoscalar meson, respectively.

Sometimes a momentum cutoff regularization scheme is also used to solve the Bethe-Salpeter equation in the unitary coupled-channel approximation. Thus the expression for G_l is given by [38]

$$\begin{aligned}G_l &= {\rm i}\int\frac{{\rm d}^4q}{(2\pi)^4}\frac{1}{2E_l(\vec{q})}\frac{1}{P^0-q^0-E_l(\vec{q})+i\epsilon}\frac{1}{q^2-m_l^2+i\epsilon}\\ &\rightarrow\int_{|\vec{q}|<q_{\max}}\frac{d^3q}{(2\pi)^3}\frac{1}{2\omega_l(\vec{q})}\frac{1}{2E_l(\vec{q})}\frac{1}{P^0-\omega_l(\vec{q})-E_l(\vec{q})+i\epsilon}\end{aligned} \tag{14}$$

with P^0 the total energy of the system, and $\omega_l(\vec{q})$, $E_l(\vec{q})$ the energies of intermediate mesons and baryons, respectively.

It is believed that the maximum momentum $q_{\max}$ should be approximately equal to the regularization scale μ in the dimensional regularization scheme, and it has been proved that these two schemes always give similar properties of the resonant state in the meson-meson and meson-baryon interaction if we set $q_{\max}\approx\mu$, just as done in Refs. [39–42].

In this work, the $B\bar{K}$ and $B_s\pi$ interaction is studied by solving the Bethe-Salpeter equation using the loop functions in Eq. (12) and Eq. (14).

5 Results

The leading order and next-to-leading order potentials between the B meson and the pseudoscalar meson in different channels are depicted in Fig. 1. It is apparent that only in the channel of $B\bar{K}\to B_s\pi$ is the leading order potential attractive, while it is zero in the channels of $B\bar{K}\to B\bar{K}$ and $B_s\pi\to B_s\pi$, as shown in Table 1. The next-to-leading order correction results in a repulsive potential in the channels of $B\bar{K}\to B\bar{K}$ and $B_s\pi\to B_s\pi$, and in the crossing channel $B\bar{K}\to B_s\pi$, the next-to-leading order Lagrangian gives a correction to the leading order potential.

If only the leading order potential of the B meson and the pseudoscalar meson in Eq. (8) is taken into account in the unitary coupled-channel approximation, a pole of the squared amplitude $|T|^2$ appears at $5567+i16$ MeV in the complex energy plane with a momentum cutoff $q_{\max}=3000$ MeV, according to the loop function in Eq. (14). Moreover, in the dimensional regularization scheme, a pole of the squared amplitude $|T|^2$ is generated dynamically at $5569+i16$ MeV if we set the subtract constant $a=-2$ and the regularization scale $\mu=3100$ MeV. It is apparent that the pole might be associated with the $X(5568)$ particle claimed by the D0 Collaboration. In addition, it is noticed that the momentum cutoff $q_{\max}$ takes a similar value to the regularization scale μ if the subtraction constant $a=-2$ is fixed.

If the next-to-leading order correction to the pseudoscalar meson and B meson potential is taken into account, a pole can be found at $5632+i25$ MeV in the complex energy plane with $a=-2$ and $\nu=3100$ MeV. Apparently, the real and imaginary parts of the pole are far away from the mass and decay width of the $X(5568)$ particle, respectively, so the subtraction constant or the regularization scale has to be adjusted. If we increase the value of the regularization scale μ, while the subtract constant a is fixed, the real and imaginary parts of the pole position both decrease. A pole of the squared amplitude $|T|^2$ at $5570+i11$ MeV is generated dynamically with $a=-2$ and $\mu=3700$ MeV in the dimensional regularization scheme. However, in order to produce a pole in the same energy region with the loop function in Eq. (14), the momentum cutoff $q_{\max}$ must be improved. Actually, with $q_{\max}=4500$ MeV, a pole of $|T|^2$ appears at $5568+i10$ MeV in the complex energy plane. Obviously, the value of $q_{\max}$ in the momentum cutoff regularization scheme is far larger than the μ value in the dimensional regularization scheme if the next-to-leading order correction to the potential of the B meson and the pseudoscalar meson is considered.

The pole position of the squared amplitude and the couplings of the resonant state to $B\bar{K}$ and $B_s\pi$ channels are listed in Table 3. The label "LO+Dim" denotes the results calculated by using the leading order potential of the B meson and the pseudoscalar meson in the dimensional regularization scheme, while the label "LO+Cutoff" stands for the results calculated by using the leading order potential in the momentum cutoff regularization scheme. The cases where the next-to-leading order correction is included in these two kinds of regularization schemes are labeled as "NLO+Dim" and "NLO+Cutoff", respectively. From Table 3, the pole position is above the $B_s\pi$ threshold and on the second Riemann sheet, and can be regarded as a resonant state of $B_s\pi$. Moreover, the couplings of the resonant state to the $B\bar{K}$ and $B_s\pi$ channels in the dimensional regularization scheme take almost the same values as those in the momentum cutoff regularization scheme. Additionally, this resonant state couples more strongly to the $B\bar{K}$ channel. Even if the next-to-leading order corrections of the B meson and the pseudoscalar meson are taken into account, the coupling to the $B\bar{K}$ channel is larger than the corresponding coupling to the $B_s\pi$ channel.

Table 3. Pole positions in the complex energy plane and couplings to different channels. The meanings of the labels LO+Dim, LO+Cutoff, NLO+Dim and NLO+Cutoff can be found in the text.

	LO+Dim	LO+Cutoff	NLO+Dim	NLO+Cutoff
a	−2	-	−2	-
μ or $q_{\max}$ (MeV)	3100	3000	3700	4500
pole position (MeV)	5569+i16	5567+i16	5570+i11	5568+i10
$B\bar{K}$	138+i11	140+i12	112+i7	111+i7
$B_s\pi$	120+i19	121+i20	101+i13	100+i13

6 $B^*\phi\to B^*\phi$

From the Lagrangians in Eqs. (1) and (4), the leading order and next-to-leading order potentials of the B^* meson and the pseudoscalar meson can be obtained similarly

$$V_{\rm LO(NLO)}(P^*(p_1)+\phi(k_1)\to P^*(p_2)+\phi(k_2)) \\ =-\varepsilon\cdot\varepsilon^* V_{\rm LO(NLO)}(P(p_1)+\phi(k_1)\to P(p_2)+\phi(k_2)), \quad (15)$$

where ε and ε^* are the polarization vectors of the initial and final B^* mesons, respectively. In the infinite heavy-quark limit, $\varepsilon\cdot\varepsilon^*=-1$ [43]. Thus, the potential of the B^*

meson with the pseudoscalar meson takes the same form as the potential of the B meson except that the mass of the B meson is replaced by the mass of the B^* meson.

In the leading order approximation, we find a pole at $5620+i16$ MeV with isospin $I=1$ and spin $J=1$, and we have set $a=-2$ and $\mu=3100$ MeV in the dimensional regularization scheme. If the next-to-leading order correction is taken into account, the resonant state appears at $5620+i11$ MeV with $a=-2$ and $\mu=3700$ MeV. In the momentum cutoff regularization scheme, we obtain the pole position at $5616+i16$ MeV with $q_{\max}=3000$ MeV if only the leading order potential of the B^* meson and the pseudoscalar meson is taken into account. In addition, if the next-to-leading order correction is included, a pole appears at $5616+i10$ MeV with $q_{\max}=4500$ MeV. The pole is higher than the $B_s^*\pi$ threshold and lies on the second Riemann sheet. If the claimed $X(5568)$ state with $J^P=0^+$ is confirmed, there is also a resonant state with $J^P=1^+$ and a mass around 5620 MeV.

7 Partners in the charm sector

Since the D meson mass is less than the B meson mass, the value of the regularization scale μ should be less than that of the B meson-pseudoscalar meson interaction in the dimensional regularization scheme if the subtraction constant $a=-2$ is fixed. For the charm sector of DK and $D_s\pi$, we find a pole at $2325+i65$ MeV in the leading order approximation with $a=-2$ and $\mu=1400$ MeV, while there is a pole at $2326+i57$ MeV in the complex energy plane when we include the next-to-leading order correction in the D meson-pseudoscalar meson interaction with $a=-2$ and $\mu=1800$ MeV. In the momentum cutoff regularization scheme, the pole appears at $2349+i74$ MeV with $q_{\max}=1600$ MeV if only the leading order potential is considered. Furthermore, if the next-to-leading order correction is taken into account, the pole lies at $2345+i62$ MeV in the complex energy plane if the momentum cutoff $q_{\max}=2500$ MeV. The pole position is above the $D_s\pi$ threshold and located on the second Riemann sheet, thus it might correspond to a resonant state, which is much like the $D_s^*(2317)$ particle except that the isospin $I=1$.

For the $D^*\bar{K}$ and $D_s^*\pi$ sector, the pole is lower than the $D^*\bar{K}$ threshold and appears on the second Riemann sheet. A pole of the squared amplitude $|T|^2$ is detected at $2493+i66$ MeV in the complex energy plane if the leading order potential is taken into account in the dimensional regularization scheme, where we have set $a=-2$ and $\mu=1400$ MeV. if the next-to-leading order correction is included, the pole moves to the position of $2490+i58$ MeV with $a=-2$ and $\mu=1800$ MeV. In the momentum cutoff regularization scheme, the pole is located at $2502+i72$ MeV with $q_{\max}=1600$ MeV in the leading order approximation. When the next-to-leading order correction is taken into account, the pole appears at $2501+i61$ MeV with the momentum cutoff $q_{\max}=2500$ MeV.

8 Summary

The possibility that the $X(5568)$ announced by the D0 Collaboration corresponds to a resonant state is discussed in this article. The potential of the B meson and the pseudoscalar meson was deduced both in the leading order approximation and in the leading order plus next-to-leading order approximation, then the amplitude of $B\bar{K}$ and $B_s\pi$ with isospin $I=1$ was studied in the unitary coupled-channel approximation of the Bethe-Salpeter equation. By adjusting the value of the regularization scale, we can obtain a reasonable pole of the squared amplitude which can be associated with the $X(5568)$ state.

We would like to thank Han-Qing Zheng, E. Oset and En Wang for useful discussions.

References

1 V. M. Abazov et al (D0 Collaboration), Phys. Rev. Lett., **117**: 022003 (2016)
2 S. S. Agaev, K. Azizi and H. Sundu, Phys. Rev. D, **93**: 074024 (2016)
3 W. Wang and R. Zhu, Chin. Phys. C, **40**: 093101 (2016)
4 Z. G. Wang, Commun. Theor. Phys., **66**: 335 (2016)
5 W. Chen, H. X. Chen, X. Liu, T. G. Steele and S. L. Zhu, Phys. Rev. Lett., **117**: 022002 (2016)
6 S. S. Agaev, K. Azizi and H. Sundu, Phys. Rev. D, **93**: 114007 (2016)
7 X. H. Liu and G. Li, Eur. Phys. J. C, **76**: 455 (2016)
8 Y. R. Liu, X. Liu and S. L. Zhu, Phys. Rev. D, **93**: 074023 (2016)
9 S. S. Agaev, K. Azizi and H. Sundu, Phys. Rev. D, **93**: 094006 (2016)
10 J. M. Dias, K. P. Khemchandani, A. Martínez Torres, M. Nielsen and C. M. Zanetti, Phys. Lett. B, **758**: 235 (2016)
11 Z. G. Wang, Eur. Phys. J. C, **76**: 279 (2016)
12 S. S. Agaev, K. Azizi and H. Sundu, Eur. Phys. J. Plus, **131**: 351 (2016)
13 X. G. He and P. Ko, Phys. Lett. B, **761**: 92 (2016)
14 F. Stancu, J. Phys. G, **43**: 105001 (2016)
15 T. J. Burns and E. S. Swanson, Phys. Lett. B, **760**: 627 (2016)
16 L. Tang and C. F. Qiao, Eur. Phys. J. C, **76**: 558 (2016)
17 F. K. Guo, U. G. Meissner and B. S. Zou, Commun. Theor. Phys., **65**: 593 (2016)
18 M. Albaladejo, J. Nieves, E. Oset, Z. F. Sun and X. Liu, Phys. Lett. B, **757**: 515 (2016)
19 A. Esposito, A. Pilloni and A. D. Polosa, Phys. Lett. B, **758**: 292 (2016)
20 J. X. Lu, X. L. Ren and L. S. Geng, Eur. Phys. J. C, **77**: 94 (2017)
21 F. Goerke, T. Gutsche, M. A. Ivanov, J. G. Korner,

V. E. Lyubovitskij and P. Santorelli, Phys. Rev. D, **94**: 094017 (2016)
22 S. S. Agaev, K. Azizi, B. Barsbay and H. Sundu, Eur. Phys. J. A, **53**: 11 (2017)
23 C. M. Zanetti, M. Nielsen and K. P. Khemchandani, Phys. Rev. D, **93**: 096011 (2016)
24 Y. Jin and S. Y. Li, Phys. Rev. D, **94**: 014023 (2016)
25 Q. F. Lu and Y. B. Dong, Phys. Rev. D, **94**: 094041 (2016)
26 R. Albuquerque, S. Narison, A. Rabemananjara and D. Rabetiarivony, Int. J. Mod. Phys. A, **31**: 1650093 (2016)
27 X. Chen and J. Ping, Eur. Phys. J. C, **76**: 351 (2016)
28 X. W. Kang and J. A. Oller, Phys. Rev. D, **94**: 054010 (2016)
29 C. B. Lang, D. Mohler and S. Prelovsek, Phys. Rev. D, **94**: 074509 (2016)
30 R. Chen and X. Liu, Phys. Rev. D, **94**: 034006 (2016)
31 R. Aaij et al (LHCb Collaboration), Phys. Rev. Lett., **117**: 152003 (2016)
32 CMS Collaboration [CMS Collaboration], CMS-PAS-BPH-16-002
33 F. K. Guo, C. Hanhart, S. Krewald and U. G. Meissner, Phys. Lett. B, **666**: 251 (2008)
34 M. Altenbuchinger, L.-S. Geng and W. Weise, Phys. Rev. D, **89**: 014026 (2014)
35 L. Liu, K. Orginos, F. -K. Guo, C. Hanhart and U. -G. Meissner, Phys. Rev. D, **87**: 014508 (2013)
36 J. A. Oller and U. G. Meissner, Phys. Lett. B, **500**: 263 (2001)
37 E. Oset and A. Ramos, Eur. Phys. J. A, **44**: 445 (2010)
38 E. Oset and A. Ramos, Nucl. Phys. A, **635**: 99 (1998)
39 D. Jido, J. A. Oller, E. Oset, A. Ramos and U. G. Meissner, Nucl. Phys. A, **725**: 181 (2003)
40 R. Molina, D. Nicmorus and E. Oset, Phys. Rev. D, **78**: 114018 (2008)
41 L. Geng and E. Oset, Phys. Rev. D, **79**: 074009 (2009)
42 S. Sarkar, B. X. Sun, E. Oset and M. J. Vicente Vacas, Eur. Phys. J. A, **44**: 431 (2010)
43 L. M. Abreu, D. Cabrera, F. J. Llanes-Estrada and J. M. Torres-Rincon, Annals Phys., **326**: 2737 (2011)